Oxyhalogen−Sulfur Chemistry: Nonlinear Oxidation Kinetics of Hydroxymethanesulfinic Acid by Acidic Iodate

Jonathan F. Ojo

Department of Chemistry, Obafemi Awolowo University, Ile-Ife, Osun State, Nigeria

Adenike Otoikhian, Rotimi Olojo, and Reuben H. Simoyi*

Department of Chemistry, Portland State University, Portland, Oregon 97207-0751

Received: October 16, 2003; In Final Form: January 16, 2004

The oxidation of hydroxymethanesulfinic acid, HMSA, by acidic iodate has been studied by spectrophotometric techniques. The reaction presents clock reaction characteristics in which in excess iodate conditions there is an initial quiescent period that is followed by a rapid production of iodine. The induction period before formation of iodine is inversely proportional to the iodate concentrations and the concentrations of acid to the second order. Iodide ions have a strong catalytic effect on the rate of the reaction by reducing the duration of the induction period. The stoichiometry of the reaction is dependent on the ratio of oxidant to reductant. In excess HMSA conditions the stoichiometry was deduced to be $3HOCH_2SO_2H + 2IO_3^- \rightarrow 3HCHO + 3SO_4^{2-} + 2I^- + 6H^+$ whereas in excess iodate and after prolonged standing the stoichiometry is $6IO_3^- + 5HOCH_2SO_2H \rightarrow 5SO_4^{2-} + 5HCOOH + 3I_2 + 4H^+ + 3H_2O$. The mechanism is dominated by the standard oxyiodine kinetics that involve the initial formation of the reactive oxyiodine species HIO_2 and HOI: $IO_3^- + 2H^+ + I^- \rightleftharpoons HIO_2 + HOI$. Further reactions will then occur between the organosulfur species with HOI. The direct reaction of aqueous iodine with HMSA is fast enough to be considered diffusion controlled, with a stoichiometry of $2I_2 + HOCH_2SO_2H + 2H_2O \rightarrow HCHO + SO_4^{2-} + 4I^- + 6H^+$. The facile nature of this reaction implies that HMSA and iodine cannot coexist in the reaction medium and that the end of the induction period coincides with a complete consumption of HMSA by iodate. The first 2-electron oxidation of HMSA yields a stable bisulfite addition compound, hydroxymethanesulfonic acid, HMSOA. Further oxidation of HMSOA is very slow, with the pathway involving the initial dissociation of HMSOA to HSO_3^- and HCHO. Although HSO_3^- is rapidly oxidized to SO_4^{2-}, HCHO is only slowly oxidized to HCOOH.

Introduction

This manuscript represents a continuation of our systematic series of studies aimed at elucidating the kinetics and mechanisms of oxidation of sulfur compounds by oxyhalogens ions.[1] Oxyhalogen chemistry is the most established source of nonlinear dynamics in chemistry.[2] Among these oxyhalogen-based systems are the well-known oscillatory Briggs−Rauscher[3−5] (BR) reaction and the pattern-forming Belousov−Zhabotinskyii[6] (BZ) reaction. These systems involve the reduction of an oxyhalogen species by a suitable reductant as the main driving force for the generation of nonlinear dynamical behavior. The recent involvement of sulfur chemistry in the development of novel chemical oscillatory systems has expanded by over 10-fold the numbers of known chemical systems that generate nonlinear, exotic dynamics.[7] Some of the unique features observed in sulfur-based systems include clock reaction behavior,[8,9] oligooscillatory dynamics,[10] pH-driven oscillations,[11] and chemical wave propagation.[12,13] Invariably, the reaction of oxyhalogens with sulfur compounds results in exotic dynamics.[14−16] The mechanistic and kinetics details of oxyhalogen chemistry have been exhaustively studied and are well-known.[6,17,18] Not much, however, is known about the mechanistic aspects of sulfur chemistry, and thus none of the recently discovered sulfur-based chemical oscillators[7] are as well-known as the BR and BZ systems that are dominated by oxyhalogens kinetics.

Our series of studies into the oxidation of organosulfur compounds has strongly implicated a pathway that involves the successive formation of sulfur oxo acids all the way to sulfate.[19] Though sulfenic acids are too unstable to be isolated,[20] the sulfinic and sulfonic acids of organosulfur compounds can be synthesized and used as starting reagents in the search for a generic mechanism for the full oxidation of organosulfur compounds to sulfate and an organic residue.[21,22] In this manuscript we report on a detailed kinetics and mechanistic study on the oxidation of hydroxymethanesulfinic acid by acidic iodate. From our preliminary studies, this reaction had shown bistability in flow conditions and clock reaction behavior in batch. A full understanding of these exotic dynamics is only possible after a complete elucidation of the kinetics and mechanism of the reaction that drives these exotic dynamics.

Experimental Section

Materials. Hydroxymethanesulfinic acid (monosodium salt dihydrate), HMSA (Sigma-Aldrich), potassium iodate, potassium iodide, soluble starch, sodium thiosulfate, perchloric acid 72%, sodium chloride (Fisher) were used as purchased. HMSA solutions were prepared just before use. Reaction solutions were prepared using singly distilled water. Iodine solutions were prepared by dissolving iodine crystals in distilled water and standardizing by titrating against sodium thiosulfate with freshly prepared starch as an indicator.

Methods. All experiments were carried out at 25 ± 0.5 °C and at a constant ionic strength of 1.0 M (NaCl). A few control experiments were performed in deionized water and water treated with EDTA to establish the possible catalytic effects of adventitious metal ions. The reaction dynamics were unaffected

* Corresponding author.

10.1021/jp037140q CCC: $27.50
Published on Web 03/04/2004

by these treatments. Two kinetics systems were studied: the IO_3^-−HMSA and I_2−HMSA reactions. Both reactions were monitored spectrophotometrically by following the absorbance of iodine at its experimentally determined isosbestic point of 465 nm.[23] Kinetics measurements for the slower IO_3^-−HMSA system were performed on a Perkin-Elmer Lambda 2S UV/vis spectrophotometer whereas for the faster I_2−HMSA system a Hi-tech Scientific SF61-DX2 stopped-flow spectrophotometer was used.

The stoichiometric determinations were performed in excess of IO_3^- by varying initial HMSA concentrations and evaluating excess oxidizing power (IO_3^- plus I_2(aq)) by adding excess acidified potassium iodide and titrating the liberated iodine against standard thiosulfate. The standard Tollen's reagent spot test was used for HCHO.[24] Sulfate was quantitatively analyzed (gravimetrically) as $BaSO_4$. For this procedure, reaction solutions were allowed to stand for 24 h before the addition of $BaCl_2$. The precipitate was also allowed to settle for 24 h before filtering, drying, and weighing. Excess iodate was first removed to avoid coprecipitation of $Ba(IO_3)_2$.

Results

Stoichiometry. Standardized solutions of HMSA and acidified iodate were mixed at various oxidant-to-reductant ratios in volumetric flasks. Qualitative analysis revealed complex and variable stoichiometries that are dependent on the initial amount of HMSA present at fixed oxidant concentrations. In excess HMSA conditions, the stoichiometry was determined to be

$$3HOCH_2SO_2H + 2IO_3^- \rightarrow 3HCHO + 3SO_4^{2-} + 2I^- + 6H^+ \quad (R1)$$

The formaldehyde product was confirmed by a positive qualitative test using Tollen's reagent.[24] Stoichiometry R1 was deduced at the highest $[IO_3^-]/[HMSA]$ ratio, R, possible before any I_2 is formed as one of the products. The value of R corresponding to this point was exactly $^2/_3$. In conditions of stoichiometric excess of iodate ($R > {}^2/_3$), formation of I_2 was due to the Dushman reaction[25−27] which utilizes the excess IO_3^- and the I^- formed from stoichiometry R1:

$$IO_3^- + 5I^- + 6H^+ \rightarrow 3I_2 + 3H_2O \quad (R2)$$

Figure 1a shows a graph of thiosulfate titer vs initial HMSA concentrations. By extrapolating to zero titer, where stoichiometry R1 is just satisfied with no further iodate to effect reaction R2, one obtains the ratio of 2:3 oxidant to reductant (stoichiometry R1). Excess HMSA conditions, in which the ratio was less than 2:3 did not deliver any clock reaction characteristics because at the end of stoichiometry R1 there was no iodate left to effect the formation of iodine.

In excess IO_3^-, the stoichiometry of the reaction was determined as

$$4IO_3^- + 5HOCH_2SO_2H \rightarrow 5SO_4^{2-} + 5HCHO + 2I_2 + 6H^+ + 2H_2O \quad (R3a)$$

Stoichiometry R3a was the first stoichiometry observed within the first 5 min of the reaction (see Figure 2). After further incubation of the reaction solutions, stoichiometry R3b was obtained:

$$6IO_3^- + 5HOCH_2SO_2H \rightarrow 5SO_4^{2-} + 5HCOOH + 3I_2 + 4H^+ + 3H_2O \quad (R3b)$$

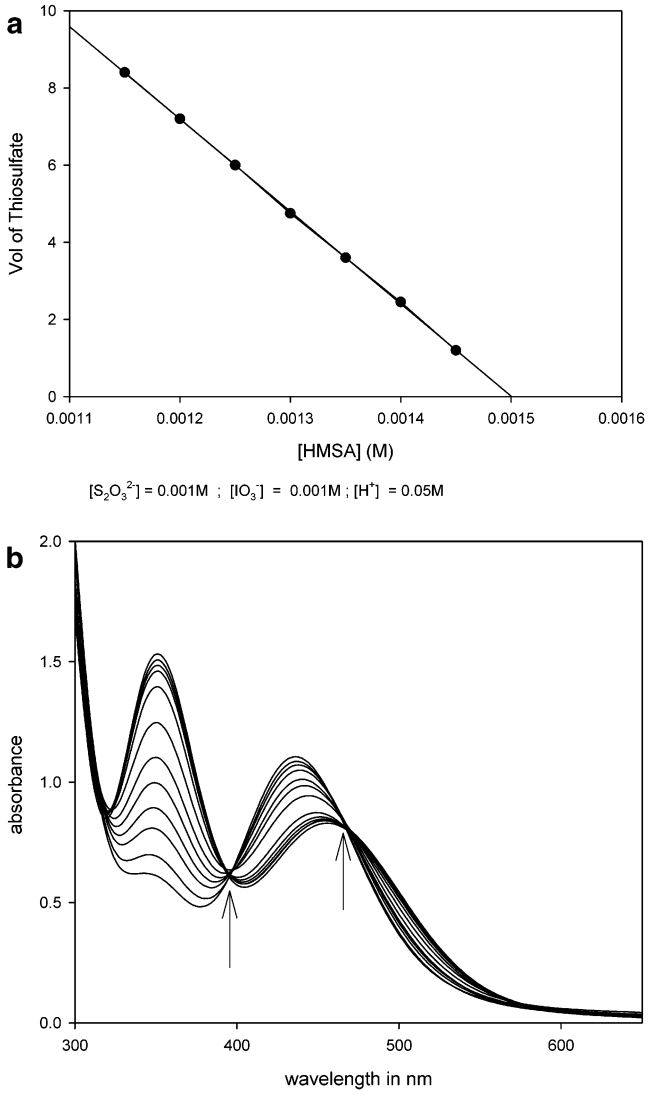

Figure 1. (a) Stoichiometric plot generated for the titration of sodium thiosulfate against available I_2 following complete oxidation of HMSA in aqueous acidic solution. (b) Two isobestic points at 395 and 465 nm generated from aqueous I_2/NaCl reaction mixture. Sodium chloride crystals are continuously added to an aqueous solution of iodine, thereby altering the ratios of I_2 to I_2Cl^-. The absorbance of the resulting solution was invariant at 395 and 465 nm.

The absence of formaldehyde (after prolonged standing of over 24 h) among the products in stoichiometry R3b was confirmed by a negative Tollen's reagent test, suggesting that any HCHO formed is later oxidized to formic acid in the presence of excess oxidant:

$$3HCHO + IO_3^- \rightarrow 3HCOOH + I^- \quad (R4)$$

Stoichiometry R3b is a composite reaction derived from a linear combination of stoichiometries R1, R2, and R4. The reaction under study involves an initial stoichiometric combination, 5R1 + 2R2, which gives formaldehyde (stoichiometry R1), followed by a further reaction that involves the oxidation of formaldehyde to formic acid. The overall stoichiometry R3b is given by the linear combination 5R1 + 3R2 + 5R4.

A separate stoichiometric determination was made for the I_2−HMSA reaction. The reaction was very fast, approaching diffusion control, with quantitative formation of sulfate, as determined by gravimetric analysis. The stoichiometry of the reaction was also dependent on the oxidant-to-reductant ratio.

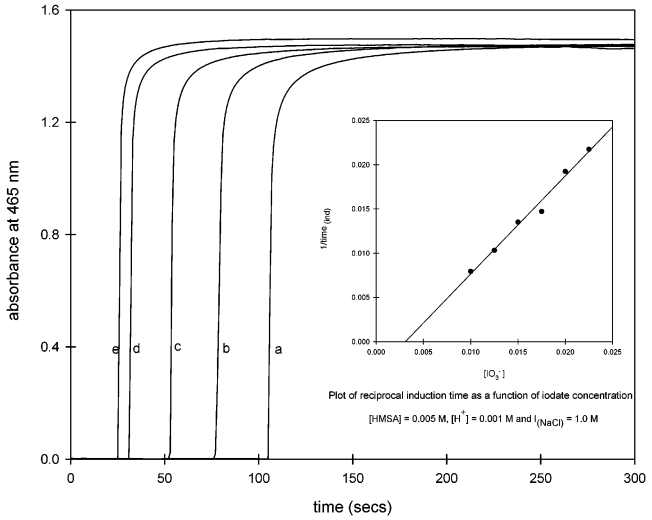

Figure 2. Variation of $[IO_3^-]_0$ in the oxidation of HMSA by iodate. $[IO_3^-]$ = (a) 0.010 M, (b) 0.0125 M, (c) 0.0150 M, (d) 0.020 M, and (e) 0.0225 M. [HMSA] = 0.005 M, $[H^+]$ = 0.001 M, and I_{NaCl} = 1.0 M.

In excess HMSA the stoichiometry was experimentally determined to be

$$2I_2 + HOCH_2SO_2H + 2H_2O \rightarrow HCHO + SO_4^{2-} + 4I^- + 6H^+ \quad (R5)$$

whereas, in excess iodine conditions, a further reaction occurs in which the formaldehyde is oxidized to formic acid:

$$HCHO + I_2 + H_2O \rightarrow HCOOH + 2I^- + 2H^+ \ (\text{slow}) \quad (R6)$$

giving an overall stoichiometric ratio of 3:1. This 3:1 stoichiometry was achieved after prolonged standing of over 72 h. Within the time scale of our experimental observations, however, iodine solutions were inert to formaldehyde.

Reaction Dynamics

The kinetics of the oxidation of HMSA by iodate could be followed by utilizing the absorption peaks at either 286, 353, or 465 nm. The first two wavelengths correspond to the triiodide species, I_3^-, whereas the peak at 465 nm is due to aqueous I_2. Some concern was raised at the use of chloride for adjusting the ionic strength due to the well-known I_2/I_2Cl^- equilibrium:[28]

$$I_2(aq) + Cl^- \rightleftharpoons I_2Cl^- \qquad K_{eq} = 2.3 \qquad (R7)$$

The establishment of the equilibrium is faster than the time scale of the iodate−HMSA reaction, and so equilibrium R7 did not interfere with the reaction under study. Further, we investigated the effect of chloride on the absorption spectrum of aqueous iodine species and derived the spectral scans shown in Figure 1b. These were obtained by successively adding carefully measured amounts of solid crystals of NaCl to an aqueous saturated iodine solution. This kept pushing the equilibrium of R7 to the right. This experiment gave two isosbestic wavelengths for the I_2/I_2Cl^- mixture at 395 and 465 nm. We thus settled with using 465 nm as the observation wavelength for all our experiments. Fortuitously, 465 nm was also our experimentally determined isosbestic point for the I_2/I_3^- equilibrium. Because no oxidation of chloride is thermodynamically feasible in this environment, no further calculations were needed to evaluate effective iodine concentrations for data acquisition performed at 465 nm. Control experiments were also performed with $NaClO_4$ and Na_2SO_4 for ionic strength adjustment with no changes observed in the reaction's global dynamics.

All IO_3^-−HMSA reactions in excess IO_3^- conditions ($R > {}^2/_3$) were characterized by a quiescent induction time followed by rapid formation of I_2 until a saturation value is reached. The initial reagent concentrations control both the duration of the induction period as well as the maximum iodine concentrations obtained.

Iodate Dependence. The magnitude of the induction time was inversely proportional to the initial iodate concentrations (Figure 2 and inset). In excess iodate concentrations, the amount of iodine obtained was determined by the HMSA concentration,s which constituted the limiting reagent. The amount of I_2 expected from stoichiometry R3a is 0.002 M, much higher than a normal saturated iodine solution of approximately 0.001 M. Without the use of NaCl for maintaining a constant ionic strength, iodine crystals would be expected to precipitate or float to the surface of the reaction solution. The use of 1.0 M chloride partitioned the molecular iodine species into 1.533×10^{-3} M I_2Cl^- and 4.667×10^{-4} M I_2(aq). The final absorbance observed is the one expected from this partitioning. The formation of iodine was extremely fast and its production was almost instantaneous at the end of the quiescent period, thus allowing a clean stoichiometric determination. Figure 2 (inset) shows a plot of reciprocal induction time as a function of $[IO_3^-]_0$. Because the minimum ratio needed before formation of iodine (as induction time $\rightarrow$ 0, inverse of induction time $\rightarrow \infty$) according to R1 is ${}^2/_3$, we expect stoichiometry R1 to be satiated by 0.003 67 M iodate. The *x*-intercept shows the minimum $[IO_3^-]_0$ concentration necessary to initiate the accumulation of I_2 at a fixed $[HMSA]_0$ is 0.0037, thus confirming stoichiometry R1. At $R < {}^2/_3$, iodate is reduced to I^- without formation of I_2 (as in reaction R2) because all available IO_3^- will be consumed in stoichiometry R1. Any iodine that is formed according to Dushman's reaction[27] in R2 is quickly consumed by the excess HMSA according to reaction R5. At higher $[IO_3^-]_0$ when $R > {}^2/_3$, the amount of I_2 produced is controlled by the amount of iodide formed in stoichiometry R1.

Acid Dependence. The concentration of acid present is a very important parameter in the overall reaction dynamics. Figure 3 shows that an increase in acid concentration shortens the (induction) time needed before the production of I_2 commences. The observed traces suggest a second-order dependence with respect to $[H^+]$, as illustrated by Figure 3 (inset) where a plot of induction time as a function of $[H^+]^{-2}$ is found to be linear. Data in the Figure 3 inset suggest that a minimum $[H^+] = 4.0 \times 10^{-4}$ M is necessary for any noticeable activity to occur via I_2 formation under conditions of excess oxidant ($R > {}^2/_3$).

HMSA Dependence. The effect of HMSA is one you would expect if the complete consumption of HMSA was a prerequisite to the formation of iodine and hence the end of the induction period. Figure 4 shows experimental results obtained by varying the amount of HMSA at fixed concentrations of $[IO_3^-]_0$ and $[H^+]_0$. The observed induction time is directly proportional to the initial concentrations of HMSA: the more HMSA present, the longer it will take for a fixed amount of iodate to completely consume. The final amount of I_2 formed is also directly proportional to $[HMSA]_0$ according to stoichiometry R3 (a and b).

Iodide Dependence. In another set of experiments, the effect of added iodide ions was studied to further understand the results observed in HMSA dependence. Figure 5 reveals that the available iodide affects both the rate of HMSA oxidation as

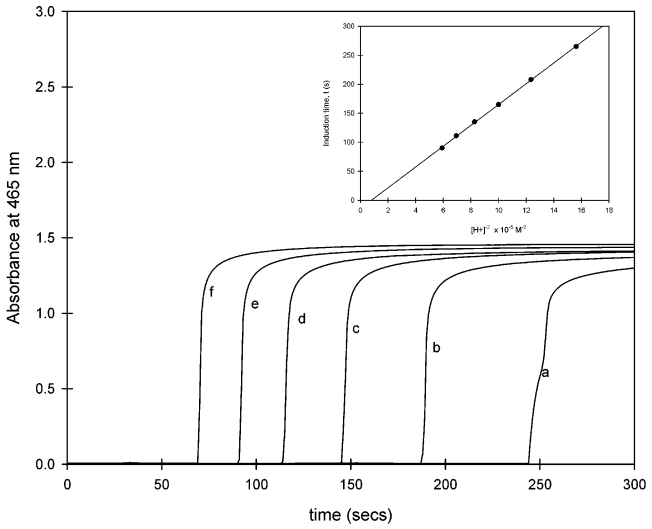

Figure 3. Variation of $[H^+]_0$ in the oxidation of HMSA by iodate. $[H^+]$ = (a) 8.0×10^{-4} M, (b) 9.0×10^{-4} M, (c) 1.0×10^{-3} M, (d) 1.1×10^{-3} M, (e) 1.2×10^{-3} M, and (f) 1.3×10^{-3} M. [HMSA] = 0.005 M, $[IO_3^-] = 0.01$M, and $I_{NaCl} = 1.0$ M. Inset: Plot of induction time as a function of $[H^+]^{-2}$.

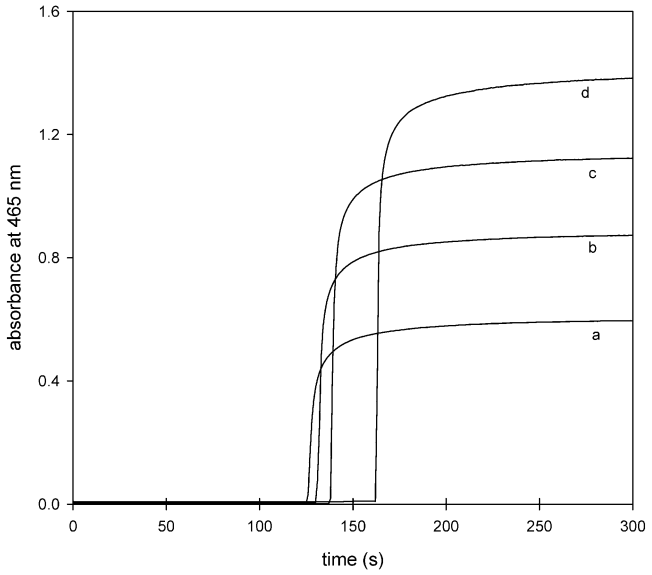

Figure 4. Variation of [HMSA] in its oxidation by iodate in aqueous acidic medium. [HMSA] = (a) 0.002 M, (b) 0.003 M, (c) 0.004 M, and (d) 0.005 M. $[IO_3^-] = 0.010$ M, $[H^+] = 0.00I1$ M, and $I_{NaCl} = 1.0$ M.

well as the final amount of I_2 produced (see inset). At fixed $[HMSA]_0$, the rate of depletion of HMSA is increased by added I^-, as evidenced by shorter induction times obtained with increasing $[I^-]_0$. Iodide is not a reactant, but it is a product that catalyzes the oxidation of HMSA by iodate. A log−log plot of the inverse of the induction period vs iodide concentration is linear with unit slope. The effect of iodide saturates as initial iodide concentrations approach and exceed the initial HMSA concentrations.

Iodine−HMSA Reaction. The reaction of iodine with HMSA is important to understand fully the mechanism of oxidation of HMSA by iodate. The direct reaction of iodine with HMSA is extremely fast, almost approaching diffusion-controlled rates. The total consumption of iodine by HMSA is essentially complete within 0.01 s, which is close to the mixing time limit of our stopped-flow spectrophotometer of 3 ms. We estimated a lower limit second-order rate constant for this

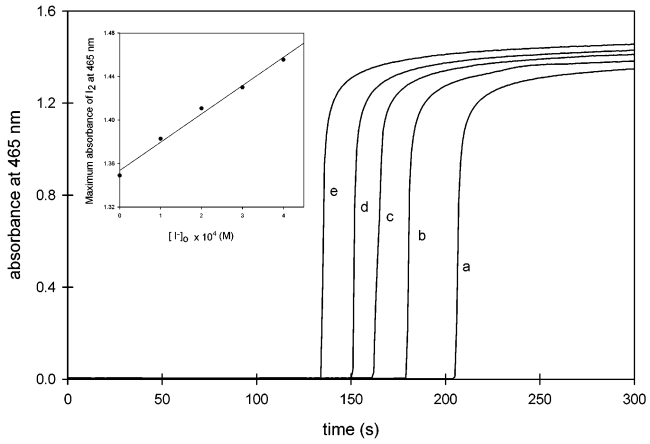

Figure 5. Variation of $[I^-]_0$ in the oxidation of HMSA by iodate in acidic solution. Fixed: $[IO_3^-] = 0.01$ M, [HMSA] = 0.005 M, $[H^+] = 8.0 \times 10^{-4}$ M, and $I_{NaCl} = 1.0$ M. $[I^-]_0$ = (a) no I^- added, (b) 1.0×10^{-4} M, (c) 2.0×10^{-4} M, (d) 3.0×10^{-4} M, and (e) 4.0×10^{-4} M. Inset: Plot of λ_{max} of I_2 as a function of $[I^-]_0$ showing linear dependence.

process as $\approx 2 \times 10^6$ M^{-1} s^{-1}. Stopped-flow traces only showed the final iodine absorbance as expected from stoichiometry R5. Decreasing HMSA concentrations in an effort to slow the reaction was ineffective. The reaction was not slowed sufficiently enough by either iodide or acid.

Further Experimental Data. Hydroxymethanesulfonic acid, HMSOA, is a well-known bisulfite-addition compound that is formed from the reaction of aqueous formaldehyde (a diol) and sodium bisulfite:[29]

$$H_2C(OH)_2 + HSO_3^- \rightleftharpoons HOCH_2SO_3^- + H_2O$$

A 2-electron oxidation of HMSA gives HMSOA. A few experiments were also performed with HMSOA as the reductant in our attempt to decipher the oxidation mechanism of HMSA. Surprisingly, the oxidation reactions of HMSOA are much slower than corresponding reactions of HMSA. Acidic HMSOA solutions reacted very slowly with iodate, and had, in previous work from this laboratory, showed no visible reaction with chlorite and chlorine dioxide.[30,31] Oxidation of HMSOA by iodine was reasonably fast, but only to as far as the formation of formaldehyde and sulfate. Further reaction of iodine and formaldehyde was exceedingly slow, and no reaction progress was observed even after allowing iodine−formaldehyde solutions to incubate for 6 h. Addition of base, which converted the aqueous iodine species to hypoiodous acid[32] delivered a much more rapid oxidation of the formaldehyde to formic acid (confirmed later by a negative Tollen's reagent test).

Mechanism

The proposed mechanism of this reaction should involve iodide as a central control species for the whole reaction scheme. Its effect is central in the production of the active reactive species HIO_2 and HOI. Only catalytic amounts of iodide are needed because every further reaction that reduces an oxyiodine species will eventually produce iodide as the lowest oxidation state of that iodine species. The initiation reaction is the slow direct reaction of HMSA with iodate to give the sulfonic acid, HMSOA, and iodous acid, HIO_2:

$$IO_3^- + HOCH_2SO_2H + H^+ \rightarrow HOCH_2SO_3H + HIO_2 \quad \text{(R8)}$$

In the absence of, or in conditions of very little, iodide, the

iodous acid will progressively be reduced all the way to iodide:

$$HIO_2 + HOCH_2SO_2H \rightarrow HOCH_2SO_3H + HOI \quad (R9)$$

$$HOI + HOCH_2SO_2H \rightarrow HOCH_2SO_3H + H^+ + I^- \quad (R10)$$

The production of iodide brings into prominence the most important reaction in this mechanism. This reaction produces the oxidizing species HIO_2 and HOI:[33]

$$IO_3^- + 2H^+ + I^- \rightleftharpoons HIO_2 + HOI \quad (R11)$$

The accumulation of iodide makes reaction R11 the rate determining step to the whole reaction scheme. Standard iodate solutions contain about 10^{-6} M iodide ions, which can initiate reaction R11, and the presence of substantial amounts of iodide ions at the beginning of the reaction will shunt out reactions R8−R10 and immediately render reaction R11 rate-determining. This has been observed in the data shown in Figure 5 where addition of very small quantities of iodide significantly reduced the induction period of the reaction. (This effect, as noted before, quickly saturated as iodide ions were continuously increased past the initial concentrations of HMSA used).

Clock Reaction Behavior. The global reaction dynamics showing clock reaction behavior arises from a delicate balance between reactions R1, R2, and R5. Reaction R5 is the fastest reaction of the three, and thus for as long as there still exists HMSA in reaction mixture, any iodine formed by reaction R2 will be immediately consumed via reaction R5. As soon as HMSA is depleted, iodine is produced, and the reaction "clocks".

Autocatalytic Production of Iodide. The observed squared acid dependence on the rate of reaction (as measured by the variation in induction period) clearly indicates that reaction R8, though it is the initiator, is not, ultimately, the rate-determining step. The only way a shift in the control of the rate of reaction from R8 to R11 can occur is if there is a nonlinear production of iodide, either through quadratic or cubic autocatalysis. A major oxyiodine reaction in solution involves the very rapid reaction of iodide and iodous acid:[34]

$$HIO_2 + I^- + H^+ \rightleftharpoons 2HOI$$
$$k_f = 2.0 \times 10^9\ M^{-3}\ s^{-1};\ k_r = 90\ M^{-1}\ s^{-1} \quad (R12)$$

Because this reaction is fast, in the presence of iodide ions, the direct oxidation of the reducing substrates in solution by iodous acid can be ignored, and hypoiodous acid used exclusively as the reactive oxidizing species in which its rate of production, as determined by the rate law derived from eq R11, becomes the rate-determining step. We can then write, in general form, the oxidation by HOI as follows:

$$HOI + \text{Red.} \rightarrow \text{Ox.} + I^- + H^+ \quad (R13)$$

where Red. is any reducing species in solution (HMSA, HMSOA ($HOCH_2SO_3H$), and HCHO) and Ox is any oxidized species after removal of 2 electrons (HMSOA, HCHO, and HCOOH). If we add R11 + R12 + 3R13, we obtain the following composite reaction in which there is cubic autocatalysis in the production of iodide:

$$IO_3^- + 2I^- + (3)\text{Red.} \rightarrow (3)\text{Ox.} + 3I^- \quad (R14)$$

Thus only small amounts of iodide ions are needed to initiate the reaction because, as the reaction proceeds, more iodide is formed until the production of iodide no longer becomes the rate-determining step, as reaction R11 takes over this role.

Formation of Iodine. The reverse reaction of the well-known disproportionation of iodine in aqueous solutions is the only pathway for the production of iodine:[32]

$$HOI + I^- + H^+ \rightleftharpoons I_2(aq) + H_2O \quad (R15)$$

Reactions R11 and R15 compete for the iodide ions produced in composite reaction R14. Reaction R15, with a forward rate constant of $3.1 \times 10^{12}\ M^{-2}\ s^{-1}$ is the fastest reaction in the reaction medium, and one expects immediate formation of iodine unless there is concomitantly an equally fast reaction that consumes iodine. This, indeed, is the case because the reaction of iodine with HMSA is essentially diffusion-controlled:

$$I_2 + HOCH_2SO_2H + H_2O \rightarrow HOCH_2SO_3H + 2I^- + 2H^+ \quad (R16)$$

$$I_2 + HOCH_2SO_3H + 2H_2O \rightarrow HCHO + SO_4^{2-} + 2I^- + 4H^+ \quad (R17)$$

In excess iodine conditions, the slower reaction R6 will then take over and oxidize HCHO to HCOOH. Data in Figures 3−5 show an instant and rapid formation of iodine at the end of the induction period, which suggests that reactions R16 and maybe R17 are so rapid that the total consumption of the sulfinic and sulfonic acids is a prerequisite for the formation of iodine. Reaction R16 was too rapid to be detected by our stopped-flow spectrophotometer. Because reactions were run in an excess of HMSA, reaction R17 could be slow and this would not be experimentally detected because the rate of reaction is monitored by the rate of consumption of the iodine-containing species.

Effect of Iodide. Figure 5 shows a very strong catalytic effect of iodide on the whole reaction scheme. This shows that the reaction is iodide-controlled. The increase in the final aqueous iodine concentrations observed (see Figure 5 inset) is justified through the enhancement of the iodide concentrations involved in reaction R2 (Dushman reaction).[33] The decrease in induction period can be attributed to the increased rate of autocatalytic production of iodide ions and immediate viability (at $t = 0$) of rate-determining reaction R11. The log−log plot of the inverse induction period and iodide ions gave a slope of unity, indicating that iodide is involved in the rate-determining step to the first power. This is what is predicted by the assumption that reaction R11 is rate-determining.

Overall Reaction Mechanism. The reaction scheme takes into account all the possible reactions involved in the oxidation of HMSA.

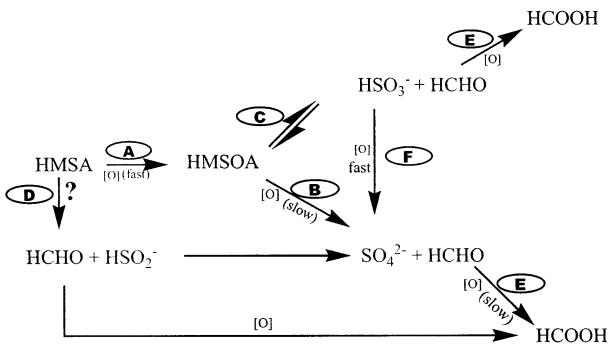

Here the oxidants, IO_3^-, HIO_2, HOI, and I_2, are collectively represented as [O], with the majority of oxidations being performed by HOI and I_2. The very rapid initial oxidation of

HMSA to HMSOA has been experimentally proved in this mechanism from the rapid diffusion-controlled oxidation of HMSA by aqueous iodine (route A). After formation of HMSOA, pathways B and C will be kinetically indistinguishable if the forward rate constant of route C is greater than the rate of reaction route B. In this case, route C's equilibrium will not affect the overall rate of reaction because reaction F is known to be very fast.[35] The inertness of HMSOA to acidic iodate suggests that the reaction predominantly goes through process C + F to produce sulfate and HCHO (stoichiometry R3a). Process D has been investigated by observing the hydrolysis of HMSA in acidic environments and was found to be negligible. In contrast, in basic environments, HMSA rapidly hydrolyzes under aerobic conditions to produce dithionite via a sulfoxyl anion radical.[36−38]

$$HOCH_2SO_2H + OH^- \rightarrow HOCH_2SO_2^- + H_2O \quad (R18)$$

$$HOCH_2SO_2^- \rightarrow HCHO + HSO_2^- \quad (R19)$$

HSO_2^- is a precursor for the formation of dithionite.[37] We can conclude, then, that under this strongly acidic environment, the major pathway for the oxidation of HMSA is A + C + F + E, with E being very slow. The formation of iodine after the induction period is much faster than one would expect from pure Dushman reaction-dominated kinetics. This would suggest that there exists a very rapid precursor reaction that rapidly produces the reaction species, HOI and I^- needed for the formation of iodine (reaction R15). The oxidation of HSO_3^- to SO_4^{2-} would present such a reaction that would enhance the autocatalytic production of I^- and H^+:

$$HSO_3^- + HOI \rightarrow SO_4^{2-} + 2H^+ + I^- \quad (R20)$$

$$HSO_3^- + I_2 + H_2O \rightarrow SO_4^{2-} + 2I^- + 3H^+ \quad (R21)$$

Process E is accomplished mainly through hypoiodous acid, HOI, and negligibly through aqueous I_2:

$$HCHO + HOI \rightarrow HCOOH + H^+ + I^- \quad (R22)$$

Computer Simulations. The important reactions in this mechanism can be compiled into Table 1. The overall reaction scheme is a simple network made up of only 15 reactions. The first reaction is the initiation reaction, which slowly builds up the reactive oxyiodine species (M1). This reaction becomes progressively less important as the reaction proceeds and iodide ions are built up (autocatalytically). It can be neglected in conditions in which we have more than 1×10^{-4} M iodide ions at the beginning of the reaction. However, in conditions in which no iodide ions are initially added to the reaction mixture, the model is very sensitive to the kinetics constants used for this reaction. Three reactions that follow in this table are the well-known oxyiodine reactions (M2−M4). The iodide-triiodide reaction (M5), though normally very important, was ineffective in this mechanism because no discernible iodide inhibition was observed in the direct reaction of iodine and HMSA. By assuming fast reaction R12 (reaction M3 in the table), we can distill the oxidation−reduction reactions to only 6, which represent a combination of two oxidants (HOI and I_2) and three reductants ($HOCH_2SO_2H$, $HOCH_2SO_3H$, and HCHO). These 6 reactions (M6, M11−M15) are made essentially irreversible because their equilibria lie overwhelmingly to the right. Imbedded inside reactions M11 and M14 are reactions M7−M10. The experimental data suggest that M11 and M14 by themselves represent a minor route to the oxidation of HMSOA. Indeed, shutting them down completely (assigning rate constants of zero) did not significantly alter the observed global dynamics of the reaction system (induction period, rate of formation of iodine, etc). Inclusion of reactions of the type R9 increased the stiffness of the integration but did not alter the observed fit. This is why we never involved the oxidations of iodous acid in our mechanism.

TABLE 1[a]

reaction no.	reaction	k_f; k_r
M1	$IO_3^- + HOCH_2SO_2H + H^+ \rightarrow HOCH_2SO_3H + HIO_2$	500
M2	$IO_3^- + 2H^+ + I^- \rightleftharpoons HIO_2 + HOI$	1.44×10^3; 2.8
M3	$HIO_2 + I^- + H^+ \rightleftharpoons 2HOI$	2.0×10^9; 90
M4	$HOI + I^- + H^+ \rightleftharpoons I_2(aq) + H_2O$	3.1×10^{12}; 2.2
M5	$I_2(aq) + I^- \rightleftharpoons I_3^-(aq)$	6.2×10^7; 8.5×10^4
M6	$HOI + HOCH_2SO_2H \rightarrow HOCH_2SO_3H + H^+ + I^-$	1.0×10^6
M7	$HOCH_2SO_2H + H_2O \rightleftharpoons HSO_3^- + HCHO + H^+$	5.0×10^3; 3.9×10^{10}
M8	$HSO_3^- + I_2 + H_2O \rightarrow SO_4^{2-} + 2I^- + 3H^+$	1.7×10^9
M9	$HSO_3^- + I_3^- + H_2O \rightarrow SO_4^{2-} + 3I^- + 3H^+$	1.5×10^7
M10	$HSO_3^- + HOI \rightarrow SO_4^{2-} + 2H^+ + I^-$	1.0×10^9
M11	$HOI + HOCH_2SO_3H + H_2O \rightarrow HCHO + SO_4^{2-} + 3H^+ + I^-$	1.0×10^2
M12	$HCHO + HOI \rightarrow HCOOH + H^+ + I^-$	1.5×10^2
M13	$I_2 + HOCH_2SO_2H + H_2O \rightarrow HOCH_2SO_3H + 2I^- + 2H^+$	2.0×10^6
M14	$I_2 + HOCH_2SO_3H + 2H_2O \rightarrow HCHO + SO_4^{2-} + 2I^- + 4H^+$	5.0×10^2
M15	$I_2 + HCHO + H_2O \rightarrow HCOOH + 2H^+ + 2I^-$	5.0×10^{-3}

[a] Except where water is involved, the order of the reaction is derived from its molecularity. For reversible reactions, the forward and reverse reactions are separated by a semicolon.

Estimating of Rate Constants Used in the Simulations. Reaction M1's forward rate constant was estimated from the best fit to the induction period. The value of 500 M^{-2} s^{-1} could also be reduced to a second-order rate constant after assuming that acid concentrations were constant. The value used, then, changed with initial acid concentrations. In conditions in which iodide ions were initially added to the reaction mixture, the simulations became insensitive to any variations in k_{M1}. Kinetics parameters for reactions M2 and M3 were derived from literature values that were adapted from the study of the Dushman[33] reaction. There were several other previous manuscripts that reported the same kinetics parameters for M2 and M3. These values were not altered nor adjusted. Reaction M4's parameters were derived from the work of Kustin and Eigen.[32] The laser-Raman spectroscopy studies of the I_2/I_3^- equilibrium performed independently by Ruasse and by Turner were the sources for the kinetics parameters used for reaction M5.[39,40] Parameters for M6 and M13 were estimated from this study. M6 was made slightly less than the estimated diffusion-controlled oxidation of HMSA by iodine. Many atmospheric chemistry studies on the bisulfite-addition compound of sulfur dioxide and formaldehyde have reported that the equilibrium constant for adduct formation[29] in the vicinity of pH 4 is approximately 7.8×10^6 M^{-1} s^{-1}. Thus, after an appropriate value of k_{M7} was guessed, the reverse was then set by the equilibrium constant. Kinetics parameters for reactions M8−M11 were derived primarily from the work of Margerum et al.[35] as well as other manuscripts written on the Landolt reaction.[31] For as long as $k_{M7} > k_{M11}$, k_{M14} the simulations became insensitive to variations in k_{M11} and k_{M14}. This was maintained throughout most of the simula-

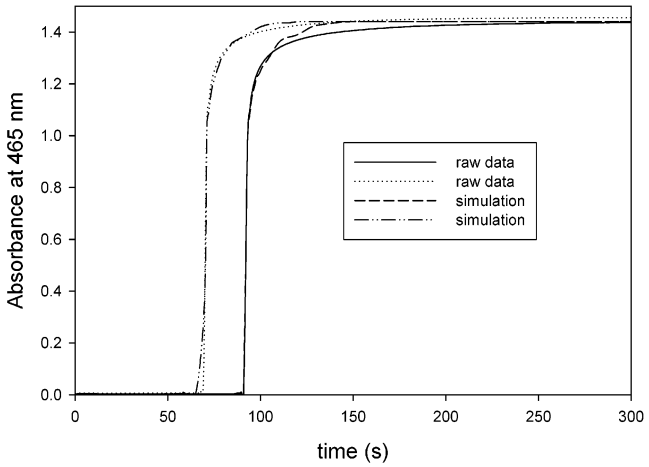

Figure 6. Computer simulations of the acid dependence data shown in Figure 3e,f. This model gave a reasonably good fit to the experimental data in both the induction period and the amount of iodine obtained at the end of the induction period.

tions performed. No special efforts were expended in trying to discern accurate values for k_{M12} and k_{M15}. Our simulations did not attempt to simulate the 3 day period that would involve the eventual quantitative oxidation of HCHO to HCOOH. The mechanism in Table 1 was able to satisfactorily model the induction period as well at its response to acid (see Figure 6) and to iodate concentrations. The model's only flaw was that it could not reproduce the very rapid rate of formation of iodine after the induction period without the use of high values for k_{M7}.

Acknowledgment. We thank Obafemi Awolowo University for awarding sabbatical leave to J.F.O. We thank Edward Chikwana for creating the ChemDraw figures for us. This work was supported by Research Grant Nos. CHE 0137435 (Bioinorganic Chemistry) and CHE 035148 (International Programs) from the National Science Foundation.

References and Notes

(1) Mambo, E.; Simoyi, R. H. *J. Phys. Chem.* **1993**, *97*, 13662−13667.
(2) Noyes, R. M. *J. Am. Chem. Soc.* **1980**, *102*, 4644−4649.
(3) Ait, A. O.; Vanag, V. K. *Zh. Fiz. Khim.* **1996**, *70*, 1385−1390.
(4) Lalitha, P. V. N.; Ramaswamy, R. *Collect. Czech. Chem. Commun.* **1992**, *57*, 2235−2240.
(5) Vukojevic, V.; Sorensen, P. G.; Hynne, F. *J. Phys. Chem.* **1993**, *97*, 4091−4100.
(6) Szalai, I.; Oslonovitch, J.; Forsterling, H. D. *J. Phys. Chem. A* **2000**, *104*, 1495−1498.
(7) Simoyi, R. H. *J. Phys. Chem.* **1986**, *90*, 2802−2804.
(8) Chinake, C. R.; Mundoma, C.; Olojo, R.; Chigwada, T.; Simoyi, R. H. *Phys. Chem. Chem. Phys.* **2001**, *3*, 4957−4964.
(9) Simoyi, R. H.; Epstein, I. R.; Kustin, I. *J. Phys. Chem.* **1994**, *98*, 551−557.
(10) Jones, J. B.; Chinake, C. R.; Simoyi, R. H. *J. Phys. Chem.* **1995**, *99*, 1523−1529.
(11) Rabai, G.; Orban, M.; Epstein, I. R. *J. Phys. Chem.* **1992**, *96*, 5414−5419.
(12) Martincigh, B. S.; Simoyi, R. H. *J. Phys. Chem. A* **2002**, *106*, 482−489.
(13) Martincigh, B. S.; Chinake, C. R.; Howes, T.; Simoyi, R. H. *Phys. Rev. E* **1997**, *55*, 7299−7303.
(14) Doona, C. J.; Stanbury, D. M. *J. Phys. Chem.* **1994**, *98*, 12630−12634.
(15) Hauser, M. J. B.; Chinake, C. R.; Simoyi, R. H. *S. Afr. J. Chem.* **1995**, *48*, 135−141.
(16) Orban, M.; De Kepper, P.; Epstein, I. R. *J. Phys. Chem.* **1982**, *86*, 431−433.
(17) Lopez-Cueto, G.; Ostra, M.; Ubide, C. *Anal. Chim. Acta* **2001**, *445*, 117−126.
(18) Sortes, C. E.; Faria, R. B. *J. Braz. Chem. Soc.* **2001**, *12*, 775−779.
(19) Chinake, C. R.; Simoyi, R. H. *J. Phys. Chem.* **1993**, *97*, 11569−11570.
(20) Dickinson, D. A.; Forman, H. J. *Ann. N. Y. Acad. Sci.* **2002**, *973*, 488−504.
(21) Makarov, S. V.; Mundoma, C.; Penn, J. H.; Petersen, J. L.; Svarovsky, S. A.; Simoyi, R. H. *Inorg. Chim. Acta* **1999**, *286*, 149−154.
(22) Makarov, S. V.; Mundoma, C.; Penn, J. H.; Svarovsky, S. A.; Simoyi, R. H. *J. Phys. Chem. A* **1998**, *102*, 6786−6792.
(23) Mundoma, C.; Simoyi, R. H. *J. Chem. Soc., Faraday Trans.* **1997**, *93*, 1543−1550.
(24) Fieser L. F. *Organic Experiments*, 2nd ed.; Lexington, MA, 1968; p 134.
(25) Rabai, G.; Kaminaga, A.; Hanazaki, I. *J. Phys. Chem.* **1995**, *99*, 9795−9800.
(26) Schmitz, G. *Phys. Chem. Chem. Phys.* **1999**, *1*, 1909−1914.
(27) Xie, Y.; McDonald, M. R.; Margerum, D. W. *Inorg. Chem.* **1999**, *38*, 3938−3942.
(28) Olsson, L.-F. *Inorg. Chem.* **1985**, *24*, 1398−1405.
(29) Deister, U.; Neeb, R.; Helas, G.; Warneck, P. *J. Phys. Chem.* **1986**, *90*, 3213−3217.
(30) Chinake, C. R.; Olojo, O.; Simoyi, R. H. *J. Phys. Chem. A* **1998**, *102*, 606−611.
(31) Gaspar, V.; Showalter, K. *J. Am. Chem. Soc.* **1987**, *109*, 4869−4876.
(32) Kustin, K.; Eigen, M. *J. Am. Chem. Soc.* **1962**, *84*, 1355−1359.
(33) Liebhafsky, H. A.; Roe, G. M. *Int. J. Chem. Kinet.* **1971**, *11*, 693−701.
(34) Urbansky, E. T.; Cooper, B. T.; Margerum, D. W. *Inorg. Chem.* **1997**, *36*, 1338−1344.
(35) Yiin, B. S.; Margerum, D. W. *Inorg. Chem.* **1989**, *29*, 1559−1564.
(36) Makarov, S. V.; Mundoma, C.; Svarovsky, S. A.; Shi, X.; Gannett, P. M.; Simoyi, R. H. *Arch. Biochem. Biophys.* **1999**, *367*, 289−296.
(37) Svarovsky, S. A.; Simoyi, R. H.; Makarov, S. V. *J. Phys. Chem. B* **2001**, *105*, 12634−12643.
(38) Svarovsky, S. A.; Simoyi, R. H.; Makarov, S. V. *J. Chem. Soc., Dalton Trans.* **2000**, 511−514.
(39) Ruasse, M.-F.; Aubard, J.; Galland, B.; Adenir, A. *J. Phys. Chem.* **1986**, *90*, 4382−4388.
(40) Turner, D. H.; Flynn, G. W.; Sutin, N.; Beitz, J. V. *J. Am. Chem. Soc.* **1972**, *94*, 1554−1559.